Measurements and Calibration of Tropospheric Delay at Goldstone from the Cassini Media Calibration System

S. J. Keihm,[1] A. Tanner,[1] and H. Rosenberger[2]

One and one-half years of near-continuous measurements of the troposphere-induced path delay at Goldstone have been analyzed in order to (1) characterize the troposphere-delay fluctuations in a statistical sense and (2) evaluate the path-delay calibration performance of the Media Calibration System (MCS) at DSS 25. Both the wet and dry components of delay are considered. Statistics based on 5-minute-interval MCS data indicate wet-delay temporal structure function (the expectation value of delay differences versus the time interval) values of 1 mm at 5 minutes, 5 mm at 1 hour, and 2 cm at 1 day, increasing to an asymptotic level of 3 to 4 cm for time scales greater than 2 days. At time scales of 1000 to 10,000 seconds, Allan standard deviation (ASD) computations of the wet-delay variations indicate slightly higher fluctuation levels than shown in a previous study. The differences are attributable to the inclusion of cloudy conditions in the present study. The dry-delay fluctuation levels are approximately one-third the wet-delay levels at all time scales from minutes to weeks.

The ability of the MCS to accurately calibrate the delay fluctuations was assessed by comparing side-by-side results from the two redundant instrumentation sets that comprise the MCS. Based on data during the first three Cassini radio science experiments, the MCS surpasses the requirement of the Cassini Gravitational Wave Experiment (residual ASD $< 1.1 \times 10^{-15}$ s/s) at all time scales >1000 seconds. For time scales extending out to weeks, the MCS has demonstrated a precision better than 0.06 cm for monitoring zenith-equivalent delay variations during spacecraft-tracking operations.

---

[1] Microwave Experiment Systems and Technology Section.

[2] Interferometry Systems and Large Optical Systems Section.

The research described in this publication was carried out by the Jet Propulsion Laboratory, California Institute of Technology, under a contract with the National Aeronautics and Space Administration.

I. Introduction

Precision spacecraft radio science and radio astronomy experiments have been used in many geophysical, planetary, and astronomical investigations. The time scales of interest vary widely depending on the phenomena being studied, e.g., [1–4]. In particular, some planetary occultations, planetary and satellite gravity-determination flybys, and relativity experiments have observations where the duration of the signal is $>10^4$ seconds [5,6]. To analyze the data and evaluate the ultimate sensitivity of these observations requires an understanding of the statistics of the competing noises on these time scales. Instrumental noises often can be made extraordinarily small, leaving propagation noise—e.g., phase scintillation in the Earth's troposphere—as an important remaining noise source for experiments having time scales from 10^2 to 10^6 seconds and longer. Utilizing data from the newly deployed Media Calibration System (MCS), this article addresses the statistics of wet and dry tropospheric phase scintillation at Goldstone, California, on time scales of minutes to multiple days, and evaluates the MCS performance in measuring variations in the line-of-sight fluctuations during the first three Cassini radio science experiments.

During the summer of 2001, the MCS was deployed at Goldstone's DSS 25 for the primary purpose of providing state-of-the-art measurements of the wet troposphere path delay in support of the 2001 to 2004 Cassini radio science experiments. The primary instruments of the redundant MCS are two Advanced Water Vapor Radiometers (AWVRs) deployed 35 m apart at DSS 25 (Fig. 1). The AWVRs measure sky brightness temperatures at three frequencies near the 22-GHz water vapor line and were designed at JPL to provide order-of-magnitude improvement in stability and precision relative to standard WVRs [7]. Their operating characteristics are summarized in Table 1. The MCS also includes two Microwave Temperature Profile (MTP) radiometers operating in the 50- to 60-GHz oxygen band and two surface meteorology packages consisting of temperature, pressure, humidity, and wind-speed sensors. The data sets are processed as redundant systems, designated system 1 and system 2, each consisting of the combined measurements from one of the two AWVRs, MTPs, and surface meteorology sensors. Details describing the basis for instrument selection and retrieval algorithm development can be found in [8].

Since September 1, 2001, the MCS has provided a near-continuous archive of radiometer and surface meteorology data. During the Cassini radio science experiments, the AWVRs track the Cassini spacecraft

Fig. 1. One of the two Advanced Water Vapor Radiometers at DSS 25.

Table 1. Characteristics of the Advanced Water Vapor Radiometer.

Characteristic	Value
Operating frequencies	22.2, 23.8, 31.4 GHz
Bandwidths	500 MHz (all channels)
Beam sizes (half-power beam width)	1.0 deg (22.2- and 23.8-GHz channels); 1.2 deg (31.4-GHz channel)
Elevation-pointing accuracy	±0.1 deg absolute (all sky)
Elevation-pointing precision	±0.01-deg stability over 1000 s

in order to provide the DSS-25 Doppler tracking data analysis with line-of-sight calibration of the tropospheric wet delay at time scales of seconds to hours. During the remaining 80 percent of the time, the AWVRs operate in a "tipping curve" mode in which a spiraling sequence of elevation/azimuth directions are sampled, with observations within one degree of zenith occurring approximately every 5 minutes. For purposes unrelated to Cassini radio science support, AWVR zenith brightness temperatures (TBs) at 5-minute intervals have been routinely extracted from the AWVR data archives, providing near-continuous TB time series since September 2001. When operating in the Cassini tracking mode, zenith brightness temperatures were obtained by a simple air-mass conversion dependent on the 5-minute-interval elevation position of the AWVRs.

The tropospheric-delay statistics presented in this article are derived from the MCS data archive of September 2001 to March 2003. Most of the wet-delay statistics are computed from the 5-minute-interval zenith TBs provided by the AWVRs. The dry-delay statistics are computed primarily from an archive of 5-minute-interval surface pressure measurements using a single sensor. The 19-month interval includes three Cassini radio science experiments: the Gravitational Wave Experiments (GWE_I and GWE_{II}) from November 26, 2001, to January 4, 2002, and from December 6, 2002, to January 14, 2003; and the Solar Conjunction Experiment (SCE_I) from June 6, 2002, to July 5, 2002. During these experiments, comparisons of the redundant instrument measurements provide an estimate of the MCS performance for calibrating both wet and dry tropospheric delay variations over time scales of 30 seconds to multiple days.

In Section II of this article, the path-delay statistics of the 19-month archive are assessed using a variety of measures, including temporal structure functions, Allan standard deviation (ASD) [9], and spectral analysis. In Section III, comparisons are made between the 19-month archive and the statistics derived from each of the Cassini radio science experiments. MCS performance also is evaluated, using comparisons between the redundant components of the system. In Section IV, results are summarized with recommendations for future work.

II. Nineteen-Month Path-Delay Statistics

A. Wet- and Dry-Delay Time Series

The MCS data utilized to compute zenith path-delay time series over the September 2001 to March 2003 interval were the three-channel AWVR brightness temperatures (for the wet component) and surface pressure (for the dry component). The wet-delay algorithm consisted of an all-weather statistical retrieval based on radiosonde-derived linear correlations between the wet-delay and AWVR zenith brightness temperatures:

$$PD_{\text{wet}} = -0.849 - 0.1364 * TB22.2 + 0.6899 * TB23.8 - 0.3062 * TB31.4 \quad (1)$$

with PD_{wet} defined as the zenith delay in centimeters due to water vapor, and the three-channel AWVR brightness temperatures (TBs) are in kelvins. A 1980 to 1988 radiosonde data archive from Desert Rock, Nevada, was used to generate the Eq. (1) coefficients by regression. Desert Rock was chosen for its elevation and climatological similarity to Goldstone. This algorithm is not as precise as the more sophisticated algorithms used during Cassini radio science experiments, but is completely adequate for the purpose of generating path-delay statistics. The zenith dry-delay algorithm is based on the assumption of hydrostatic equilibrium [10] and is specific to the latitude and elevation of DSS 25 at Goldstone:

$$PD_{\text{dry}} = 0.22789 * P_s \tag{2}$$

with PD_{dry} defined as the zenith dry delay in centimeters, and P_s is the measured surface pressure in millibars.

The 19-month PD_{wet} archive was derived primarily from the system-1 AWVR data, with system-2 data used to fill in gaps when the system-1 AWVR was off line. The completeness of the combined data set was such that only four gaps greater than 2 hours remained in the PD_{wet} time series. Linear interpolation was used to complete the final 5-minute-interval archive. For the PD_{dry} archive, the uninterrupted 5-minute January 2002 to March 2003 interval P_s data from a single surface meteorology package were used in the Eq. (2) conversion. A total of three surface meteorology packages were employed during the 19-month interval. The single longest consecutive running P_s measurement was used to generate the PD_{dry} statistics in order to avoid intercalibration issues.

Figures 2 and 3 show the final time series of DSS-25 zenith wet and dry delays obtained from the MCS data using Eqs. (1) and (2). Note that the variability of the much larger dry-delay component is only $\sim$1/3 that of the wet delay. This result is consistent in all considered metrics of the wet- and dry-delay variations. An annual variation is seen in both the wet- and dry-delay time series, but this component has little impact on the time scales of interest to radio science experiments. Figures 4 (wet) and 5 (dry) show compressed versions of the time series over 10-day intervals of summer and winter, illustrating shorter time scale effects. A diurnal component is seen, most clearly in the dry-delay time series, and most persistently during summer months. The summertime dry-delay component also shows a semi-diurnal feature. The dry-delay diurnal variations are most likely related to daily wind-speed patterns.

B. Path-Delay Temporal Structure Functions

From the 19- and 15-month data sets of wet- and dry-delay time series, the expected levels of path-delay fluctuations can be computed for all time scales important for radio science experiments. We define the temporal structure function (TSF) for zenith path delay as

$$TSF(\Delta t) = \left\langle \left[PD(t + \Delta t) - PD(t) \right]^2 \right\rangle^{1/2} \tag{3}$$

where the $< >$ brackets denote an expectation value for sampling time Δt.

Application of Eq. (3) to the time series shown in Figs. 2 and 3 yields the wet and dry temporal structure functions shown in Fig. 6. The expected variations increase rapidly with the time interval out to approximately 50 hours, beyond which the variability remains nearly constant, with the wet component three times more variable than the dry. Month-to-month fluctuations in the 12- to 96-hour time scale wet-delay structure functions are shown in Fig. 7, illustrating the TSF variability at Goldstone. Note that, at time scales <24 hours, the seasonal variations in the wet TSF appear to be small.

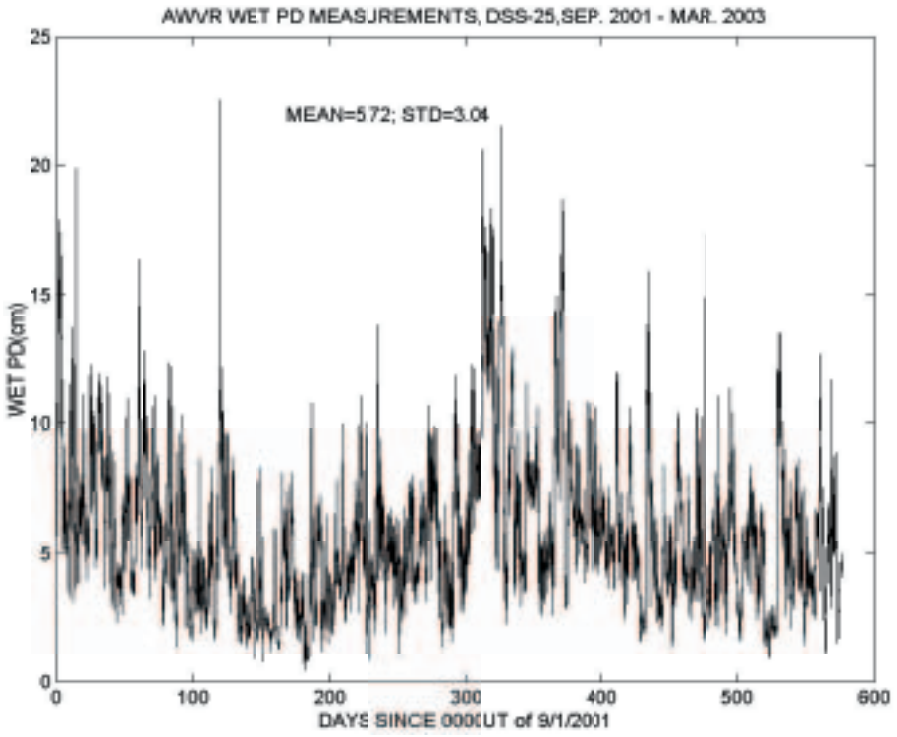

Fig. 2. Nineteen-month time series of zenith wet-delay measurements at DSS 25 from AWVR data.

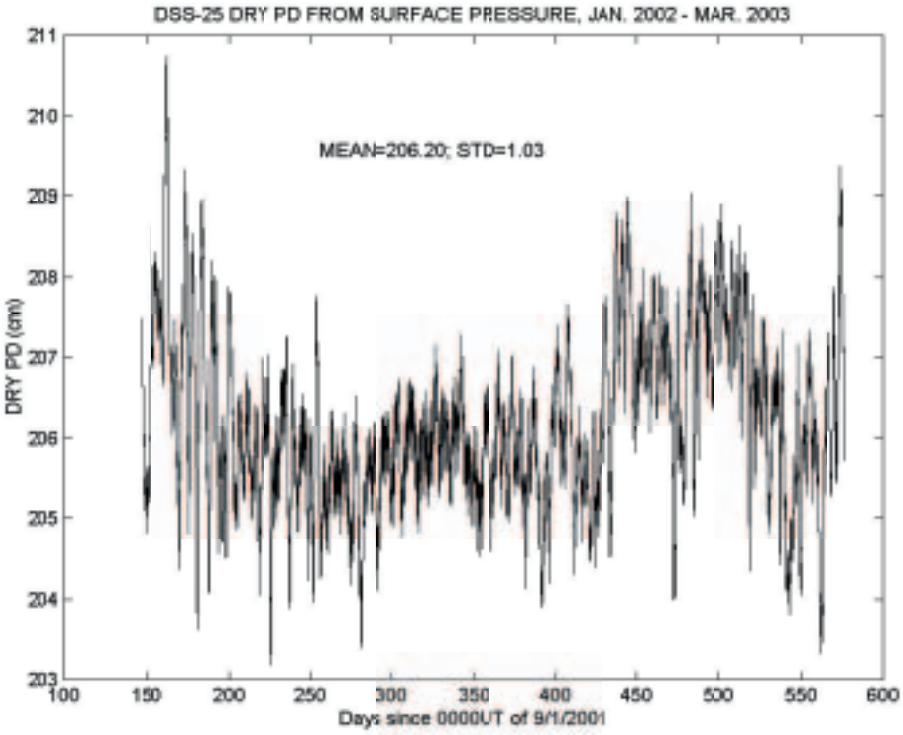

Fig. 3. Fifteen-month time series of zenith dry-delay measurements at DSS 25 from surface pressure data.

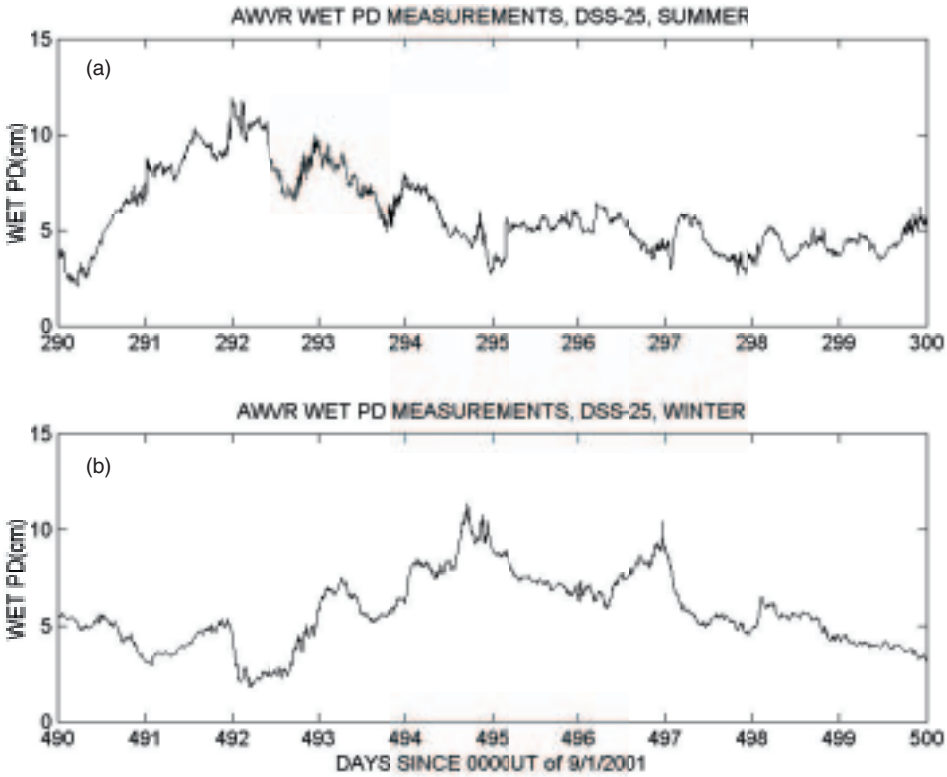

Fig. 4. Compressed-scale time series of DSS-25 zenith wet delay over 10-day (a) summer and (b) winter intervals.

C. Allan Standard Deviation Statistics

At time scales relevant to sidereal tracking, the Allan standard deviation (ASD) of delay is frequently used as a measure of the non-linear fluctuation levels of the tropospheric delay:

$$ASD(\Delta t) = \frac{\left\langle \left[\tau(t) - 2\tau(t+\Delta t) + \tau(t+2\Delta t)\right]^2 \right\rangle^{1/2}}{\left[\sqrt{2}\cdot\Delta t\right]} \tag{4}$$

where $\tau(t)$ is the delay in seconds at time t and Δt is a time interval increment. Equation (4) defines a statistical quantity which is proportional to the second-order variability of the delay over time interval Δt. The time delay τ is obtained from the PD measurements simply by dividing by the speed of light.

As an example, the MCS performance requirement for the Cassini Gravitational Wave Experiment [11] is that the ASD of the residual troposphere-induced delay (after calibration) be less than 1.1×10^{-15} s/s over time intervals of 1000 to 10,000 seconds. As an indicator of MCS performance requirements, the uncalibrated ASD spectra, computed from the 19- and 15-month time series of wet and dry zenith delays at DSS 25, are shown in Fig. 8 over time intervals from 5 minutes to 10 hours. The dry-delay ASD spectrum reveals that expected fluctuation levels fall below (meet) the GWE requirement at the 1000- to 10,000-s time scales. However, the ASD of the tropospheric wet delay can be expected to exceed (fail) the GWE requirement by a factor of three to seven at zenith, increasing rapidly at lower elevation angles in proportion to air mass. Comparison of the expected levels of tropospheric-delay fluctuations with the GWE requirements indicates that the MCS system must remove (calibrate) approximately 90 percent or more of the wet-delay ASD near 1000-s time scales.

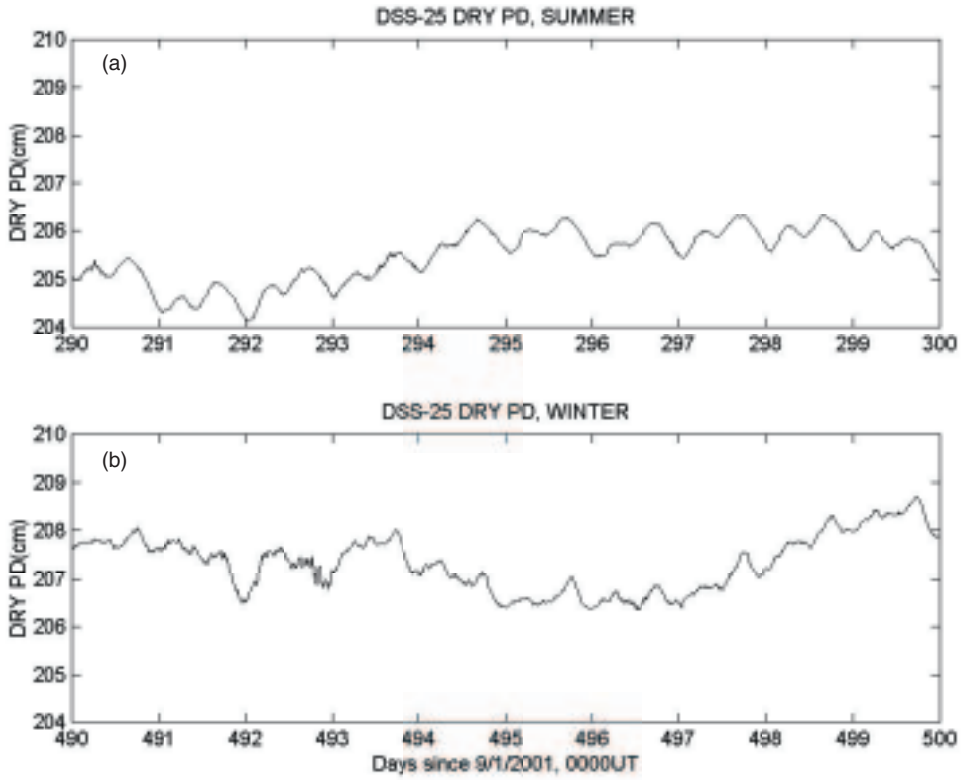

Fig. 5. Compressed-scale time series of DSS-25 zenith dry delay over 10-day (a) summer and (b) winter intervals.

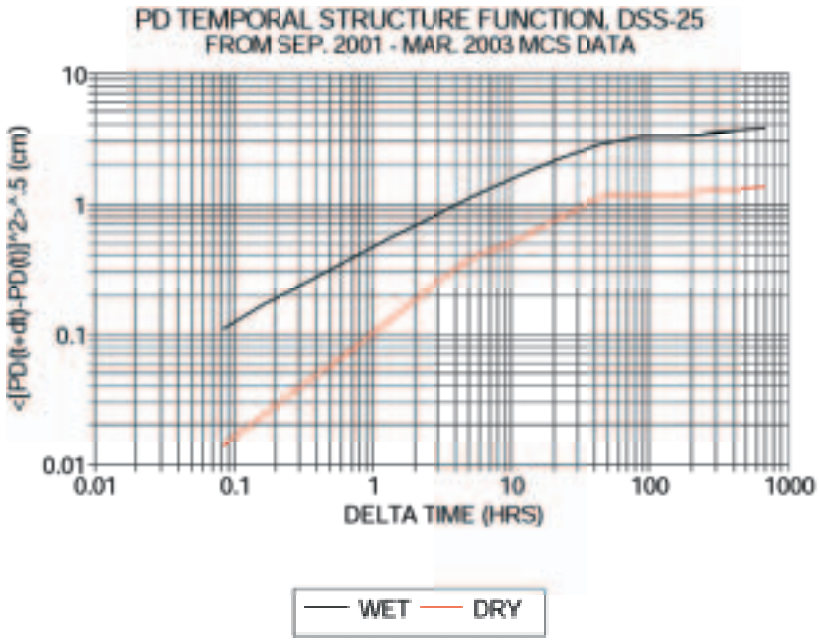

Fig. 6. Wet- (and dry)-delay temporal structure functions as measured at DSS 25 over 19- (and 14)-month intervals.

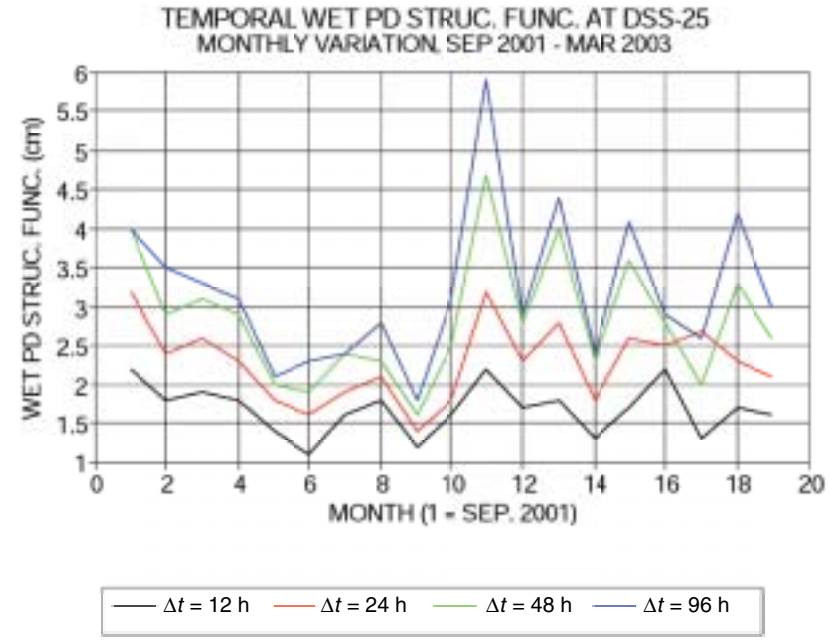

Fig. 7. Monthly variation of wet-delay temporal structure function at selected time intervals.

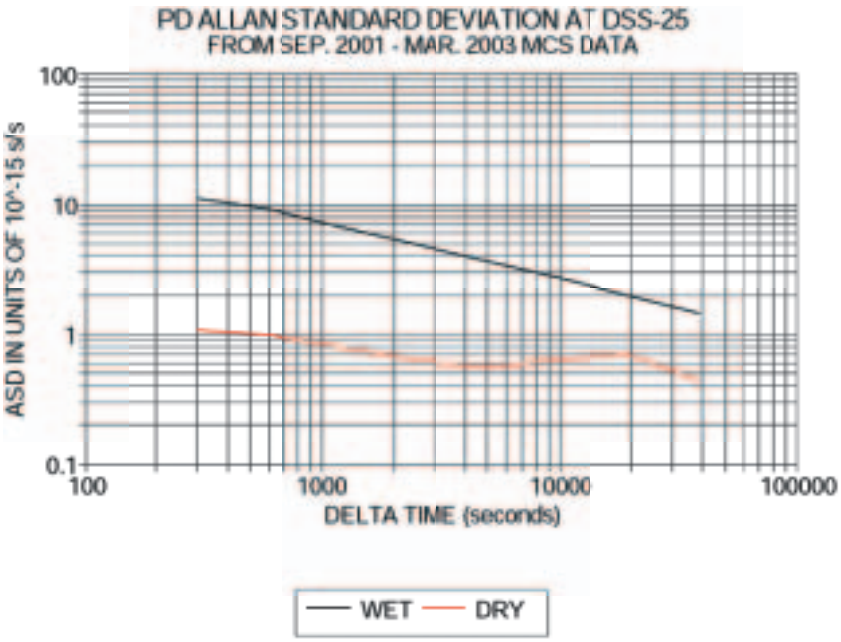

Fig. 8. Wet- (and dry)-delay Allan standard deviation as measured at DSS 25 over 19- (and 14)-month intervals.

Figure 9 shows the month-to-month variations in the wet-delay ASD statistic, featuring some seasonal dependence, most evident at the 1000-s time scale. Comparison of these results with an earlier study [12] reveals 20 to 50 percent higher ASD levels than measured during the October 1993 to September 1994 interval at DSS 13. The difference is primarily due to the inclusion of cloudy conditions in the more recent archive. The analysis of the 1993 to 1994 data included only 24-hour intervals of cloud-free data. Day/night stratification of the complete September 2001 to March 2003 data set has not been examined. However, separate analysis (Section III) of the 30- to 40-day intervals of the SCE (summer day) and GWE (winter night) MCS data reveal seasonal as well as day/night contrasts.

D. Spectral Analysis

Figures 10 and 11 show the two-sided wet- and dry-delay power spectra computed from the time series shown in Figs. 2 and 3. In the spectral analysis, the data were pre-whitened with a first-difference filter (which has zero response at DC, giving zero mean) and post-darkened after Fourier transforming. The wet spectrum is roughly power law at high frequencies, less steep than for the Kolmogorov value (blue line, $\sim f^{-2.67}$), and shows no significant diurnal or higher-frequency harmonics. As seen in the temporal structure function analysis, the spectral level of the dry delay is below that of the wet. However, the dry spectrum does contain a clear diurnal component plus higher harmonics, as suggested previously in the compressed (10-day) plots of the dry delay (Fig. 5). The diurnal-scale dry-delay (surface pressure) harmonics may be caused by repeating daily wind patterns at Goldstone.

III. MCS Statistics and Performance During Cassini Radio Science Experiments

During the Cassini gravitational wave and solar conjunction radio science experiments, the AWVRs of the MCS track the Cassini spacecraft in order to provide the best possible corrections of the line-of-sight delay fluctuations for the DSS-25 Doppler delay measurements. After final processing, the MCS data product consists of 24- to 30-second-interval time series of zenith-equivalent wet delay and surface-pressure-derived dry delay. The daily time series typically are 10 to 12 hours in duration (the Cassini

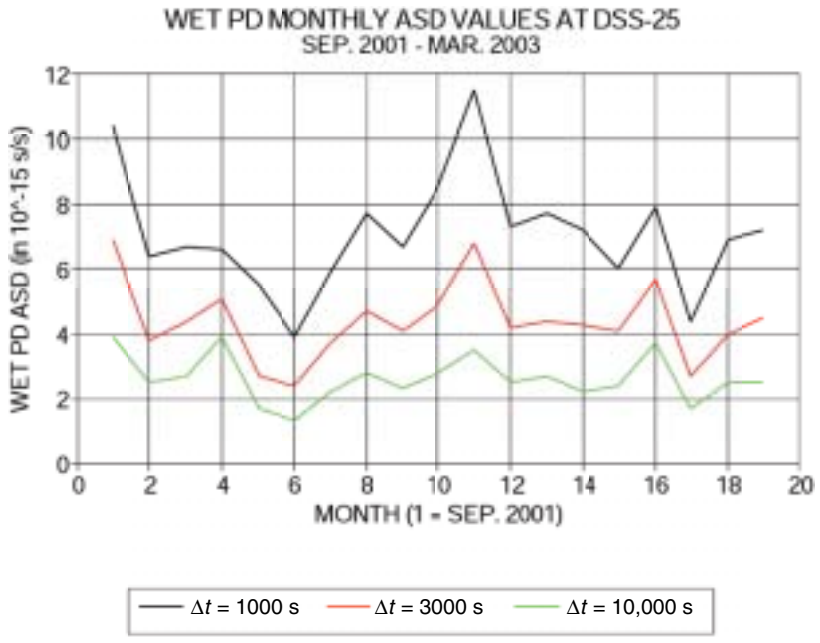

Fig. 9. Monthly variation of wet-delay Allan standard deviation at selected time intervals.

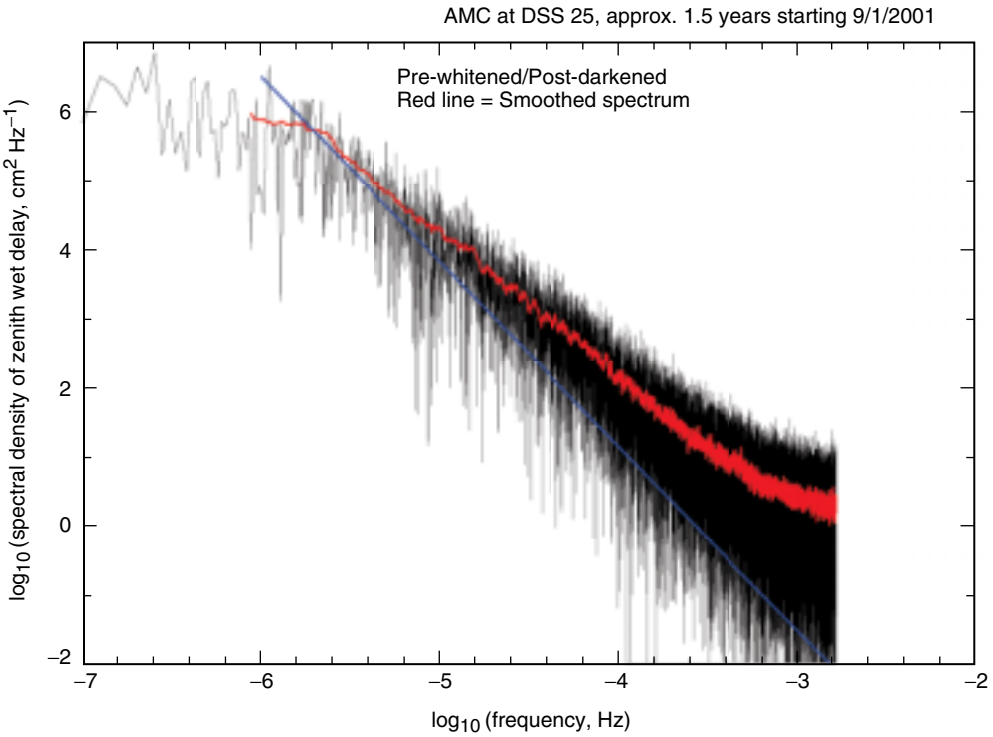

Fig. 10. Spectral density of zenith wet delay from 19-month DSS-25 measurements.

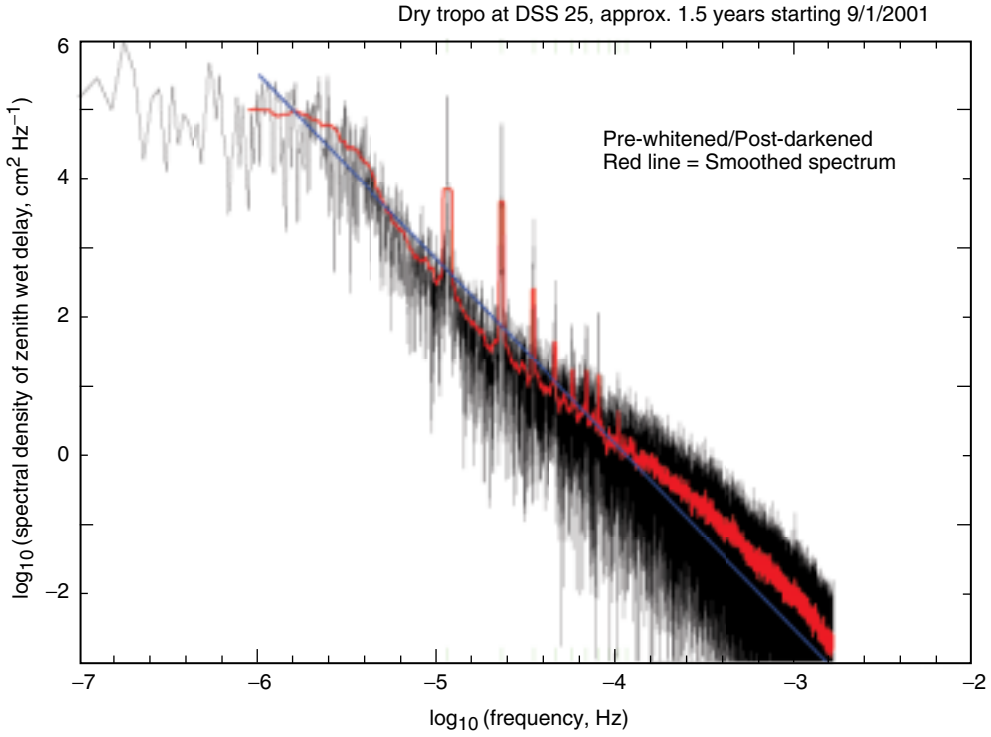

Fig. 11. Spectral density of zenith dry delay from 14-month DSS-25 measurements.

track), over nighttime hours for the 40 consecutive winter tracks of the GWEs and over daytime hours during the 30 consecutive summer tracks of the SCE. Note that the wet-delay algorithms employed during the Cassini radio science experiments are much more complex than the simple AWVR brightness temperature conversion used for the 19-month archive. The addition of MTP and surface meteorology observables is intended to maximize the precision of the path-delay-fluctuation measurements [8]. However, the use of off-nadir AWVR measurements and a more precise algorithm will have no significant effect on the zenith path-delay-fluctuation statistics that derive from the MCS data.

Because the Goldstone MCS consists of two identical sets of instruments, comparisons of the two systems' path-delay measurements during Cassini tracking provide an estimate of the precision and stability of the MCS. Primary error sources, including instrument calibration stability, AWVR elevation-pointing uncertainties, and sampled air-mass separation, are expected to be uncorrelated between the redundant systems so that the differences in the path-delay measurements provide a lower-bound error estimate for the system. Potential correlated errors, such as the absorption-model uncertainties in the wet path-delay retrieval algorithm, may be a factor for the absolute accuracy of the measurements, but are not expected to be significant for issues of precision in the measurements of the path-delay variations. The most important test of the MCS performance will result from a comparison of the MCS-derived delay fluctuations with the residual phase fluctuations (data not yet available) derived from the GWE and SCE Doppler tracking measurements. However, such comparisons also will require a quantitative evaluation of the uncertainties in the Doppler-derived phase variations before an assessment of the MCS accuracy can be made.

A. Temporal Structure Function Statistics and MCS Calibration Performance

Figures 12 and 13 show the wet and dry path-delay temporal structure function spectra computed for the first SCE (SCE_I) and the first and second GWEs (GWE_I and GWE_{II}). The solid lines indicate the uncalibrated spectra as measured by system 1. The dashed lines indicate the difference spectra (system 2 minus system 1), our estimate of tropospheric calibration performance by the MCS. (Note that in Figs. 12 and 13 and later in Figs. 15 and 16 the dashed spectra referred to as "calibrated" actually represent the residual variations of the system-differenced measurements. As discussed above, these difference spectra represent our current best estimate of the uncertainties in the MCS calibration of the tropospheric-delay fluctuations.) Because the Cassini radio science experiments are discontinuous (sidereal tracking of the spacecraft) over 30 to 40 consecutive days, the expectation spectra shown in Figs. 12 and 13 required some modifications beyond the calculation of Eq. (3). For time intervals less than 10 hours, Eq. (3) was applied to each day's MCS tracking data, and the daily results were averaged over the 30- to 40-day duration of the experiment. For time scales of 1, 2, 4, 8, and 16 days, Eq. (3) was applied to paired days of the MCS tracking data, and the results were averaged over the lifetime of each experiment.

Note first that for all three Cassini radio science experiments the measured uncalibrated wet- and dry-delay fluctuations shown in Figs. 12 and 13 are consistent with the statistics from the 19-month data set shown in Fig. 6. Small differences seen in the wet structure function statistics are consistent with a model [12] of higher fluctuation levels during summer daytime (SCE_I) relative to winter nighttime (GWE_I and GWE_{II}).

The most noteworthy aspects of the results shown in Figs. 12 and 13 are the dashed spectra of system-differenced fluctuation measurements obtained during Cassini spacecraft tracking. These spectra reflect the MCS performance for measuring changes in the tropospheric delay over time scales of 30 seconds to 16 days. For the zenith wet delay (Fig. 12), the MCS provides better than 0.06-cm calibration precision over all computed time intervals (up to 16 days). The wet-delay calibration performance is largely independent of the magnitude of the uncalibrated path-delay variations.

The dry fluctuation component (Fig. 13) is removable to a precision better than 0.01 cm for all time scales up to 16 days. The variability of the dry-delay performance is driven primarily by wind conditions.

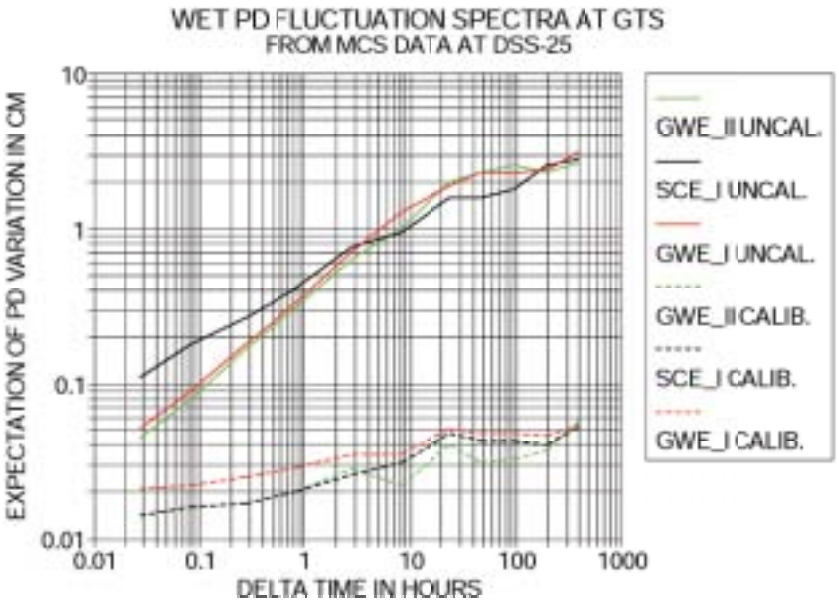

Fig. 12. Wet path-delay fluctuation spectra at DSS 25 during three Cassini radio science experiments. Solid curves indicate temporal structure function statistics of the wet troposphere before MCS calibration. Dashed curves indicate residual structure function statistics of the redundant system-differenced wet-delay measurements.

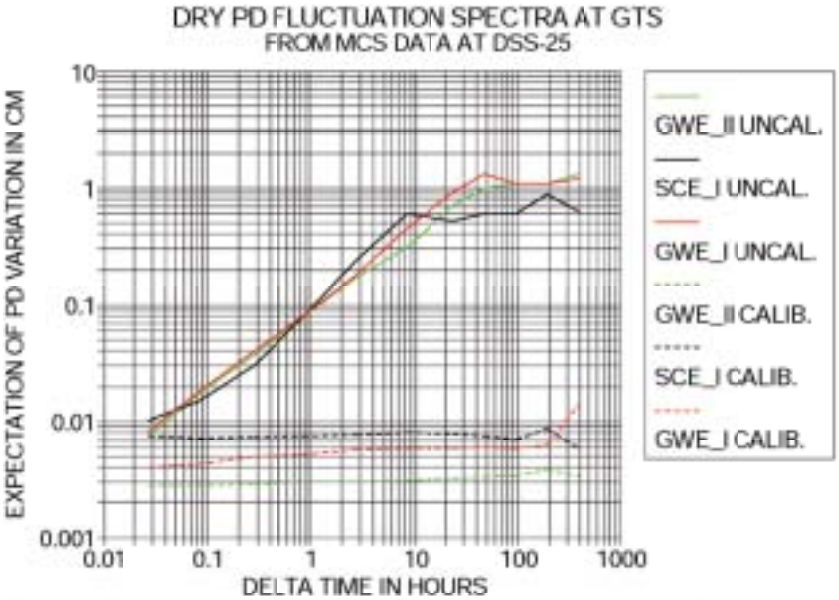

Fig. 13. Dry path-delay fluctuation spectra at DSS 25 during three Cassini radio science experiments. Solid curves indicate temporal structure function statistics of the dry troposphere before MCS calibration. Dashed curves indicate residual structure function statistics of the redundant system-differenced dry-delay measurements.

For surface wind speeds greater than 16.09 km/h (10 miles/h), small high-frequency fluctuations occur in the surface pressure measurements, which convert to a higher "noise" level in the system-differenced dry-delay component. A typical example of the correlation between the surface pressure fluctuation level and measured wind speed is shown in Fig. 14. Measurements are shown from both system-1 and system-2 surface meteorology packages during an SCE Cassini track in 2002. Note that the "worst" dry-delay calibration performance occurred for the daytime/summer SCE when higher wind conditions were most common.

B. Allan Standard Deviation Statistics and MCS Calibration Performance

Figures 15 and 16 show the wet and dry ASD spectra computed for the three Cassini radio science experiments to date. As shown previously for the temporal structure function spectra, the solid lines indicate the uncalibrated spectra as measured by system 1. The dashed lines indicate the difference spectra (system 2 minus system 1), our estimate of tropospheric calibration performance by the MCS. The computed time intervals extend from 30 to 10,000 seconds, covering the time scales of primary interest for the Cassini GWE. The computed values shown are actually 30- to 40-day averages of the values computed for each Cassini track.

Note first that the uncalibrated ASD spectra derived from MCS Cassini tracking are consistent with the 19-month spectra derived from AWVR zenith TB measurements shown in Fig. 8. Factor-of-two variations due to seasonal or day/night effects are not unexpected. For example, note the difference between the wet-delay ASD levels of the summer/daytime (SCE_I) and winter/nighttime (GWE_I and GWE_{II}) MCS data (solid curves of Fig. 15). In contrast, the calibrated wet ASD spectra, estimated by the system-2

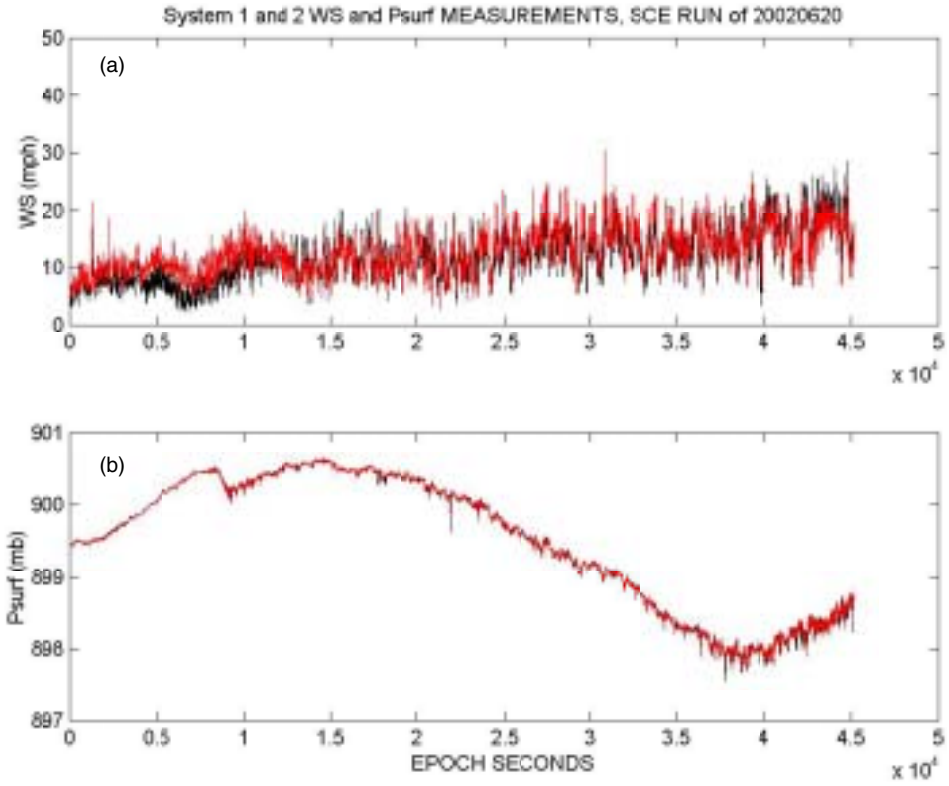

Fig. 14. Measurements of (a) wind speed and (b) surface pressure provided by the redundant MCS instruments during the June 20, 2002, Cassini tracking experiment. System-1 data in black; system-2 data in red. Note the correlation of higher wind speeds, >16.09 km/h (>10 miles/h), with increased levels of pressure measurement fluctuations.

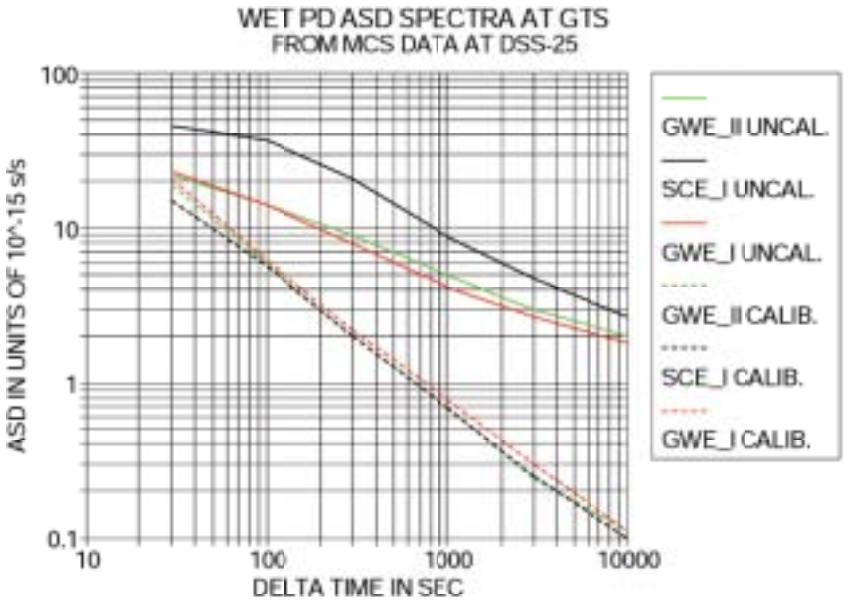

Fig. 15. Wet path-delay Allan standard deviation spectra at DSS 25 during three Cassini radio science experiments. Solid curves indicate ASD statistics of the wet troposphere before MCS calibration. Dashed curves indicate residual ASD statistics of the redundant system-differenced wet-delay measurements.

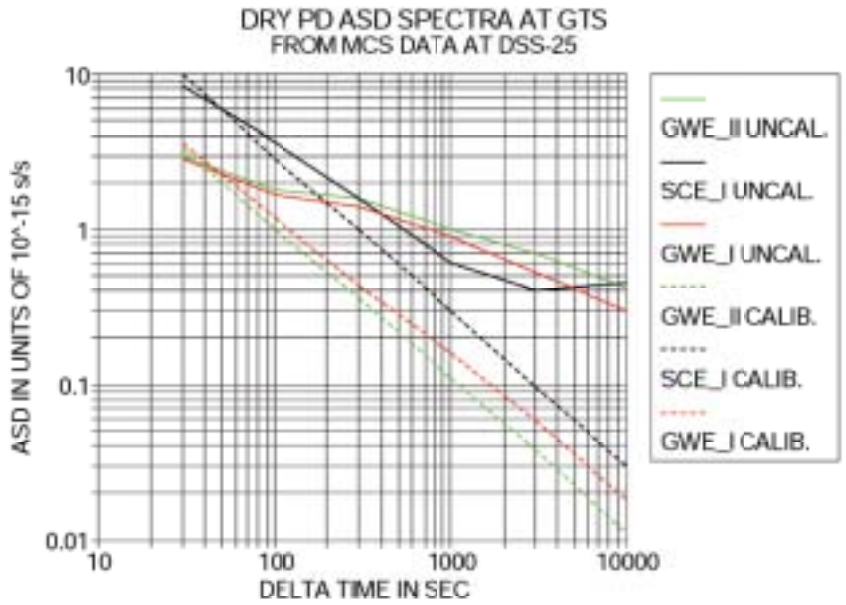

Fig. 16. Dry path-delay Allan standard deviation spectra at DSS 25 during three Cassini radio science experiments. Solid curves indicate ASD statistics of the dry troposphere before MCS calibration. Dashed curves indicate residual ASD statistics of the redundant system-differenced dry-delay measurements.

minus system-1 measured path-delay differences (dashed lines of Fig. 15), are nearly identical, indicating MCS performance that is insensitive to the actual fluctuation level in the troposphere. The calibrated (system-differenced) dashed spectra of Fig. 15 are to be compared with the GWE requirement that the residual (post-calibration) ASD for 1000- to 10,000-s time scales be less than 1.1×10^{-15} s/s. The results shown in Fig. 15 indicate that the MCS has surpassed that requirement.

The ASD spectra due to uncalibrated dry-delay fluctuations are generally 5 to 10 times smaller than the wet component (solid lines, Fig. 16), below the level of the GWE requirement for 1000- to 10000-s time scales. After calibration, as estimated by the system-differenced ASD (dashed lines), the residual dry fluctuation levels are approximately 1 to 2 orders of magnitude below the GWE requirement.

IV. Summary

Statistical properties of both wet and dry path-delay fluctuations at Goldstone have been measured over the September 2001 to March 2003 interval using instrumentation of the Media Calibration System deployed at DSS 25 in the summer of 2001. Variations have been characterized using path-delay structure functions and Allan standard deviation in the time domain and Fourier spectra in the frequency domain. For the period examined, the wet-delay fluctuation levels are 20 to 50 percent higher than computed from an earlier one-year data set, a result attributable to the exclusion of cloudy conditions in the earlier archive.

Measured dry-delay fluctuation levels are approximately one-third those of the wet component at hour and longer time scales. In the frequency domain, the dry-delay power spectrum contains significant diurnal harmonics, indicative of the effects of repeating daily wind patterns on the surface pressure measurements.

Fluctuation statistics obtained during periods of the Cassini spacecraft sidereal tracking are consistent with the results obtained using the complete 19-month archive. Factor-of-two variations are seen in the summer/daytime versus winter/nighttime wet-delay statistics, consistent with previous analysis of an earlier Goldstone WVR data archive. At a 1000-second time scale, the uncalibrated zenith wet-delay fluctuations are seen to be typically a factor of fifteen higher than the GWE specification. At 10,000 seconds, the naturally occurring wet troposphere ASD exceeds the GWE specification by a factor of two at zenith, scaling to a factor of six at 20-degree elevation. The naturally occurring dry-delay fluctuations (in the ASD domain) are typically below the Cassini GWE requirement for all time scales from 1000 to 10,000 seconds.

Comparisons of the path-delay measurements provided by the redundant systems of the MCS provide an estimate of the system's precision for calibrating line-of-sight tropospheric-delay variations during the Cassini radio science experiments. System-differenced path-delay measurements reflect error components due to limitations of instrument calibration and stability, AWVR pointing, and beam separation. In the ASD domain, the criterion used for Cassini radio science experiments, the mean residual errors produced by the system-differenced measurements fall well below (within range of) the Cassini GWE requirement at all time scales >1000 seconds. The MCS performance does not depend on the absolute or fluctuation level of the tropospheric wet delay, but does diminish for moderate to heavy cloud conditions.

The indicated MCS performance is clearly superior to the results of earlier validation tests in which the system was used to calibrate site-differenced, line-of-sight delays measured with a radio interferometer over a 21-km baseline at Goldstone [13–15]. The consensus from the earlier experiments was that the comparison tests were limited by unknown errors in the radio interferometry measurements. The current results, in which MCS precision is evaluated by the redundant system comparisons, represent the upper bound of performance (lower-bound error) in that common mode errors (modeling and algorithm) are cancelled by the system-differenced calculation. However, an earlier design study [8] demonstrated that these errors likely will be small relative to the system errors (calibration stability, pointing accuracy),

suggesting that the current optimized performance described in this article is a fair evaluation of the MCS capability.

The extraordinary stability and elevation-pointing precision of the MCS AWVRs clearly are demonstrated in the measurements of path-delay variations over multi-hour to multi-day time scales. The system-differenced measurements indicate that the 1- to 5-cm zenith wet-delay variations typical at Goldstone over time scales of days to weeks can be corrected by the MCS to precisions better than 0.06 cm. The surface pressure sensors of the MCS have demonstrated stability sufficient to produce better than 0.01-cm precision in the calibration of dry-delay variations over time scales of weeks. These results suggest that the Goldstone MCS provides a correction for greater than 95 percent of the troposphere-induced, line-of-sight propagation "noise" over minute to multi-week time scales, enabling a wide range of radio science and radio astronomy experiments.

Acknowledgments

We thank Elias Barbinis for his careful handling of the MCS data post-processing following the Cassini radio science experiments and J. W. Armstrong for his interest in the long-term delay statistics and for contributing Figs. 10 and 11. We also are grateful to the operations crew at Goldstone for all of their invaluable assistance in the deployment and maintenance of the MCS system at DSS 25. We also thank Charles Naudet for many useful comments and suggestions in his review of the manuscript.

References

[1] H. T. Howard, V. R. Eshleman, D. P. Hinson, A. J. Kliore, G. F. Lindal, R. Woo, M. K. Bird, H. Volland, P. Edenhofer, M. Patzold, and H. Porsche, "Galileo Radio Science Investigations," *Space Sci. Rev.*, vol. 60, pp. 565–590, 1992.

[2] G. L. Tyler, G. Balmino, D. P. Hinson, W. L. Sjogren, D. E. Smith, R. Woo, S. W. Asmar, M. J. Connally, C. L. Hamilton, and R. A. Simpson, "Radio Science Investigations with Mars Observer," *JGR*, vol. 97, pp. 7759–7779, 1992.

[3] S. W. Asmar and N. Renzetti, *The Deep Space Network as an Instrument for Radio Science Research*, JPL Publication 80-93 (Rev. 1), Jet Propulsion Laboratory, Pasadena, California, 1993.

[4] A. Kliore, J. D. Anderson, J. W. Armstrong, S. W. Asmar, C. L. Hamilton, N. J. Rappaport, H. D. Wahlquist, R. Ambrosini, B. Bertotti, F. M. Flasar, R. G. French, L. Iess, E. A. Marouf, and A. F. Nagy, "Cassini Radio Science Investigations," *Space Sci. Rev.* (in press), 2004.

[5] J. W. Armstrong, L. Iess, B. Bertotti, and P. Tortora, "Gravitational Wave Background: Upper Limits in the 10^{-6} to 10^{-3} Hz Band," *ApJ*, vol. 599, pp. 806–813, 2003.

[6] B. Bertotti, L. Iess, and P. Tortora, "A Test of General Relativity Using Radio Links with the Cassini Spacecraft," *Nature*, vol. 425, no. 6956, pp. 374–376, 2003.

[7] A. B. Tanner, "Development of a High-Stability Water Vapor Radiometer," *Radio Science*, vol. 33, pp. 449–462, 1998.

[8] S. J. Keihm and K. A. Marsh, "Advanced Algorithm and System Development for Cassini Radio Science Tropospheric Calibration," *The Telecommunications and Data Acquisition Progress Report 42-127, July–September 1996*, Jet Propulsion Laboratory, Pasadena, California, pp. 1–20, November 15, 1996.
http://tmo.jpl.nasa.gov/tmo/progress_report/42-127/127A.pdf

[9] D. W. Allan, "Statistics of Atomic Frequency Standards," *Proc. IEEE*, vol. 54, no. 2, pp. 221–230, February 1966.

[10] G. Elgered, "Tropospheric Radio Path Delay from Ground-Based Microwave Radiometry," in *Atmospheric Remote Sensing by Microwave Radiometry*, M. A. Janssen, Ed., New York: Wiley, 1993.

[11] M. Tinto and J. W. Armstrong, "Spacecraft Doppler Tracking as a Narrow-Band Detector of Gravitational Radiation," *Phys. Rev. D*, vol. 58, no. 042002, pp. 042002-1–042002-8, 1998.

[12] S. J. Keihm, "Water Vapor Radiometer Measurements of the Tropospheric Delay Fluctuations at Goldstone Over a Full Year," *The Telecommunications and Data Acquisition Progress Report 42-122, April–June 1995*, Jet Propulsion Laboratory, Pasadena, California, pp. 1–11, August 15, 1995.
http://tmo.jpl.nasa.gov/tmo/progress_report/42-122/122J.pdf

[13] C. Naudet, C. Jacobs, S. Keihm, G. Lanyi, R. Linfield, G. Resch, L. Riley, H. Rosenberger, and A. Tanner, "The Media Calibration System for Cassini Radio Science: Part I," *The Telecommunications and Mission Operations Progress Report 42-143, July–September 2000*, Jet Propulsion Laboratory, Pasadena, California, pp. 1–8, November 15, 2000.
http://tmo.jpl.nasa.gov/tmo/progress_report/42-143/143I.pdf

[14] G. M. Resch, J. E. Clark, S. J. Keihm, G. E. Lanyi, C. J. Naudet, A. L. Riley, H. W. Rosenberger, and A. B. Tanner, "The Media Calibration System for Cassini Radio Science: Part II," *The Telecommunications and Mission Operations Progress Report 42-145, January–March 2001*, Jet Propulsion Laboratory, Pasadena, California, pp. 1–20, May 15, 2001.
http://tmo.jpl.nasa.gov/tmo/progress_report/42-145/145J.pdf

[15] G. M. Resch, S. J. Keihm, G. E. Lanyi, R. P. Linfield, C. J. Naudet, A. L. Riley, H. W. Rosenberger, and A. B. Tanner, "The Media Calibration System for Cassini Radio Science: Part III," *The Interplanetary Network Progress Report 42-148, October–December 2001*, Jet Propulsion Laboratory, Pasadena, California, pp. 1–12, February 15, 2002.
http://ipnpr.jpl.nasa.gov/tmo/progress_report/42-148/148H.pdf